

# **SIMULATION OF SPACECRAFT CHARGING ENVIRONMENTS BY MONOENERGETIC BEAMS\***

**Ward Halverson  
Spire Corporation**

## **SUMMARY**

We have examined mathematical techniques to choose the energy and current density of monoenergetic beams to simulate the distributed spectra of plasmas in space. In the first approach, the differential current density spectrum of the plasma was divided into a number of energy bands and the beam energy and current were calculated for each band to provide a piecewise reproduction of the distributed spectrum. The second approach was to choose the beam energies and current densities to match the velocity moments of the plasma distribution function. The velocity moments are averages related to physical quantities such as particle density, flux, pressure, and energy flux, and have been used extensively to characterize the measured properties of plasmas in space. Combinations of one, two, and three beams were found to match two to six velocity moments of Maxwellian distributions. The same techniques also can be applied to other spectral shapes, and they were used to examine two-Maxwellian distributions.

A simple computational model was used to compare the charging of a spacecraft by plasmas with distributed spectra and by monoenergetic beams. These calculations were made to gain a qualitative comparison of the approaches for choosing monoenergetic beams to simulate space plasmas. Although a close comparison was not expected when only a few beams were used to simulate the distributed spectrum of a plasma, some combinations of beams gave similar charging rates and equilibrium potentials. The equilibrium potentials found using beams to match velocity moments of a two-Maxwellian plasma generally were within a few kilovolts of charging by the distributed spectrum, but showed more divergence than the simulations of simple Maxwellian plasmas.

## **INTRODUCTION**

Interactions between the plasmas in space and the surface and various subsystems of spacecraft are very complicated and have been the subject of considerable study over the past several years. Electrostatic charging,<sup>(1,2,3)</sup> for example, of a spacecraft's surface can result in discharges which can cause electromagnetic interference,

---

\*Supported by the Air Force Geophysics Laboratory.

degradation of surface materials, and failures of sensitive components. Techniques to influence plasma-spacecraft interactions, such as on-board plasma generators and conductive coatings for dielectrics, are also being actively studied.<sup>(3)</sup>

The plasma environment of space can be partially simulated in the laboratory using low-temperature plasma generators for studies of phenomena in the ionosphere and low-earth-orbit or combinations of electron and ion beams to simulate the conditions in high-altitude orbits. Several small space plasma simulation laboratories(e.g., 4) and a few large-scale facilities are in operation<sup>(5)</sup> or being planned.<sup>(6)</sup> Laboratory simulation, however, is necessarily only a partial re-creation of the actual environment to which a spacecraft is subjected.

The selection of the plasma generators or beams to simulate the space environment is now based on intuitive as well as scientific, engineering, and economic grounds. The simulation often represents only the most extreme case expected for a given spacecraft component. There are presently no established techniques for selecting a laboratory plasma environment to simulate the measured or postulated properties of plasmas in space.

The object of this work is to investigate some mathematical techniques which could be used to choose the parameters of monoenergetic beams to simulate space plasmas. The moderate temperature plasmas of geomagnetic substorms serve as examples for simulation, since they are known to cause electrostatic charging on geosynchronous satellites. The multikiloelectronvolt energies and densities of a few particles per cubic centimeter require their simulation by monoenergetic beams rather than by low-energy plasmas with a continuous energy spectrum.

## BEAM SELECTION TECHNIQUES

The plasma environment of space is characterized by a wide variety of particle energies, fluxes, species, and spectral shapes. The particle spectra vary with position in space, time, and solar activity. Models of the environment have been developed in various degrees of complexity, ranging from the definition of average plasma properties such as density and temperature at a given altitude to presentations of detailed spectra of "typical" plasma injection events recorded by instrumented satellites.

In this section we examine techniques which can be used to specify the parameters of multiple monoenergetic charged particle beams which would provide a mathematically correct and physically plausible simulation of a given plasma environment. The techniques are based on the piecewise reproduction of the shape of distributed energy spectra or by matching various averages of the velocity distribution functions by the monoenergetic beams.

In this study we assume that the space plasma to be simulated is of high enough energy and low enough density so that collective effects in the plasma can be neglected. More precisely, the Debye length of the plasma is considerably greater than typical dimensions of a spacecraft. This assumption is justified for the space environment outside the plasmasphere during geomagnetic substorms when strong spacecraft charging events are recorded.

### Piecewise Spectral Reproduction

The simplest and most obvious method to simulate a distributed spectrum is to break the spectrum into several bands and provide monoenergetic beams with appropriate currents and energies to reproduce the distribution in a "piecewise" manner. A very close reproduction of the distributed spectrum can be made in this way, provided there is a sufficient number of available beams.

With a limited number of beams, a problem arises on the choice of the energy boundaries between the parts of the spectrum to be simulated. Possible choices include fractions or multiples of the average energy (temperature) or velocity, or boundaries which divide the particle flux into equal fractions of the total flux. A given spectrum may also be divided to account for particular features, such as a high energy "tail" of the distribution function.

The principles involved in piecewise spectral reproduction can be illustrated by considering a Maxwellian distribution of particle energies. The differential energy spectrum of current density crossing an arbitrary surface is given by

$$\frac{dj}{dE} = j_0 \frac{E}{(kT)^2} \exp\left(-\frac{E}{kT}\right) \quad (1)$$

where

$$j_0 = \frac{qn}{4} \left(\frac{8kT}{\pi m}\right)^{1/2}$$

is the total current density  $q$  and  $m$  are the charge and mass of the particles.

Integrating Eq. (1) over a range of energy bounded by  $E_1$  and  $E_2$ , we find

$$j(E_1, E_2) = j_0 \left[ \left(1 + \frac{E_1}{kT}\right) e^{-\frac{E_1}{kT}} - \left(1 + \frac{E_2}{kT}\right) e^{-\frac{E_2}{kT}} \right] \quad (2)$$

This current density must be supplied by a monoenergetic beam with an energy between  $E_1$  and  $E_2$  to simulate the corresponding part of the distributed spectrum. The energy of the beam can be chosen in a number of ways; a relatively simple choice is to use the value found by averaging over the differential energy spectrum of the current density.

$$\bar{E}(E_1, E_2) = \frac{\int_{E_1}^{E_2} E \frac{dj}{dE} dE}{j(E_1, E_2)} \quad (3)$$

Integration of Eq. (3) gives,

$$\bar{E}(E_1, E_2) = \frac{j_0 T}{j(E_1, E_2)} \left\{ \left[ \left( 1 + \frac{kT}{E_1} \right)^2 + 1 \right] e^{-\frac{E_1}{kT}} - \left[ \left( 1 + \frac{kT}{E_2} \right)^2 + 1 \right] e^{-\frac{E_2}{kT}} \right\} \quad (4)$$

Table 1 gives values for  $j(E_1, E_2)/j_0$  and  $E(E_1, E_2)$  for the case of a 10 keV Maxwellian spectrum divided into four ranges of energy with boundaries at 0, 7.5, 15, and 30 keV.

### Velocity Moments

A plasma can be characterized by various averages of the velocity distributions of its constituent particles. In general, the "velocity moments" of a given distribution function,  $f(v)$ , are defined by

$$M_k = 4\pi \int_0^\infty v^k f(v) v^2 dv \quad (5)$$

$k = 0, 1, 2, \dots$

where the  $4\pi v^2 dv$  term represents an infinitesimal element in (isotropic) velocity space.

The velocity moments,  $M_k$ , can be related to physical averages for several values of  $k$ . For example,  $M_0$ ,  $M_1$ ,  $M_2$ , and  $M_3$  are related, respectively, to the average number density  $\langle N \rangle$ , particle flux,  $\langle NF \rangle$ , pressure,  $\langle P \rangle$ , and energy flux,  $\langle EF \rangle$ , of the given particle type in the plasma.

$$M_0 = \langle N \rangle = n$$

$$M_1 = 4\pi \langle NF \rangle = n \langle v \rangle = n \left( \frac{8}{\pi} \frac{kT}{m} \right)^{1/2} \quad (6)$$

$$M_2 = \frac{3}{m} \langle P \rangle = \frac{3\pi}{8} n \left( \frac{8}{\pi} \frac{kT}{m} \right)^{1/2}$$

$$M_3 = \frac{8\pi}{m} \langle EF \rangle = \frac{\pi}{2} n \left( \frac{8}{\pi} \frac{kT}{m} \right)^{3/2}$$

$$M_4 = \frac{15}{64} \pi^2 n \left( \frac{8}{\pi} \frac{kT}{m} \right)^2$$

$$M_5 = \frac{3}{8} \pi^2 n \left( \frac{8}{\pi} \frac{kT}{m} \right)^{5/2}$$

The average speed,  $\langle v \rangle$ , in equation (6) is defined by

$$\langle v \rangle = \frac{M_1}{M_0} \quad (7)$$

The expressions on the right-hand side of equation (6) are given for the case of a Maxwellian velocity distribution,

$$f(v) = n \left( \frac{m}{2\pi kT} \right)^{3/2} e^{-\frac{mv^2}{2kT}} \quad (8)$$

where  $n$ ,  $m$ , and  $T$  are respectively the number density, mass, and temperature of the particles and  $k$  is Boltzmann's constant.

A useful method for characterizing a non-Maxwellian plasma is to define effective temperatures which are related to ratios of the velocity moments.<sup>(7)</sup> The average and RMS temperatures are given by

$$T_{AV} = \frac{1}{k} \frac{\langle P \rangle}{\langle N \rangle} = \frac{m}{3k} \frac{M_2}{M_0} \quad (9)$$

$$T_{RMS} = \frac{1}{k} \frac{\langle EF \rangle}{2\langle NF \rangle} = \frac{m}{4k} \frac{M_3}{M_1} \quad (10)$$

The two temperatures are equal when the velocity distribution is Maxwellian.

#### Monoenergetic Beams to Match Velocity Moments

A technique to simulate a plasma with a distributed velocity distribution is to choose the velocities and particle densities of monoenergetic beams so that their velocity moments match those of the plasma. Under these conditions, the average parameters of the beams, such as number density, pressure, or energy flux, are equal to those of the plasma component under simulation.

In general, a single beam can match two moments of the distributed spectrum, so that two beams can match four moments, three beams, six moments, etc. As discussed later, it is also possible to overspecify the problem and use more than the minimum number of beams to match a given number of velocity moments.

A single monoenergetic beam can match two moments according to the simultaneous equations,

$$\begin{aligned} n_b v_b^j &= M_j \\ &\quad (j \neq k) \\ n_b v_b^k &= M_k \end{aligned} \quad (11)$$

where  $n_b$  and  $v_b$  are the density and velocity of the beam particles.

For example, when the zeroth (number density) and second (pressure) moments are chosen,

$$\begin{aligned} n_b &= n \\ v_b &= \left( \frac{M_2}{M_0} \right)^{1/2} = \left( \frac{3 k T_{AV}}{m} \right)^{1/2} \end{aligned} \quad (12)$$

or, in terms, of beam energy,  $E_b$ ,

$$E_b = \frac{3}{2} k T_{AV} \quad (13)$$

If the first (number flux) and third (energy flux) moments are used,

$$\begin{aligned} n_b &= \frac{M_1}{v_b} = n \langle v \rangle \left( \frac{m}{4 k T_{RMS}} \right)^{1/2} \\ v_b &= \left( \frac{M_3}{M_1} \right)^{1/2} = \left( \frac{4 k T_{RMS}}{m} \right)^{1/2} \end{aligned} \quad (14)$$

or

$$E_b = 2 k T_{RMS} \quad (15)$$

The densities and velocities of two monoenergetic beams can be found to match the zeroth through third velocity moments of the distributed spectrum by solving four simultaneous equations:

$$\begin{aligned} n_1 + n_2 &= n \\ n_1 v_1 + n_2 v_2 &= n \langle v \rangle \\ n_1 v_1^2 + n_2 v_2^2 &= \frac{3}{m} n T_{AV} \\ n_1 v_1^3 + n_2 v_2^3 &= \frac{4}{m} n \langle v \rangle T_{RMS} \end{aligned} \quad (16)$$

where  $n_1$ ,  $n_2$ ,  $v_1$ , and  $v_2$  are the densities and velocities of the beams, and the velocity moments of the distributed spectrum have been replaced by relations (7), (9), and (10). Boltzmann's constant,  $k$ , has been taken to be unity.

The velocities and densities of the monoenergetic beams can be found analytically,

$$\begin{aligned} v_{1,2} &= \frac{\langle v \rangle}{6 T_{AV} - 2 m \langle v \rangle} \cdot \left\{ 4 T_{RMS} - 3 T_{AV} \right. \\ &\quad \left. \pm \left[ 8 T_{RMS} (2 T_{RMS} - 9 T_{AV} + 2 m \langle v \rangle^2) \right. \right. \\ &\quad \left. \left. - 27 T_{AV}^2 \left( 1 - \frac{4 T_{AV}}{m \langle v \rangle^2} \right) \right]^{1/2} \right\} \end{aligned} \quad (17)$$

$$n_1 = n \left( \frac{v_2 - \langle v \rangle}{v_1 - v_2} \right) \quad (18)$$

$$n_2 = n - n_1$$

For a Maxwellian plasma, where  $T_{AV} = T_{RMS} = T$ , equation (17) simplifies somewhat,

$$v_{1,2} = \frac{\pi \langle v \rangle}{6\pi - 16} \left\{ 1 \pm \left( \frac{27}{2} \pi + \frac{128}{\pi} - 83 \right)^{1/2} \right\} \quad (19)$$

The beam densities and energies are then found to be

$$\begin{aligned} n_1 &= 0.382 n \\ n_2 &= 0.618 n \end{aligned} \quad (20)$$

$$\begin{aligned} E_1 &= 3.007 T \\ E_2 &= 0.568 T \end{aligned} \quad (21)$$

Six moments of the distributed spectrum can be used to compute the densities and velocities of three monoenergetic beams. No analytical solutions have been found for this case, but iterative techniques can be used to find solutions of the set of six simultaneous, nonlinear equations.

We have used an iterative minimization procedure<sup>(8)</sup> to find the beam velocities and densities in terms of the average speed and density of the plasma particles. For the case of a Maxwellian plasma with temperature,  $T$ , the beam densities and energies are

$$\begin{aligned} n_{1,2,3} &= [0.087, 0.588, 0.325] n \\ E_{1,2,3} &= [4.931, 1.657, 0.303] T \end{aligned} \quad (22)$$

Different values will be found for other types of velocity distribution functions, but the method used to compute the Maxwellian results is general for all realistic spectral shapes.

## Two-Maxwellian Plasmas

Garrett showed that a two-Maxwellian fit is often a good representation of plasma distribution functions measured during geomagnetic substorms.<sup>(9)</sup> The density and temperature of each Maxwellian component can be found from four velocity moments of the measured spectrum. It is possible, in principle, to find three-Maxwellian fits which match six moments, although the effects of errors in measurement of the plasma spectrum become increasingly exaggerated when computing the high-order moments. It should also be possible to find multiple-Maxwellian least-square fits directly from the measured distribution functions without computing the velocity moments of the data.

A two-Maxwellian distribution has average and RMS temperatures given by

$$T_{AV} = \frac{n_1 T_1 + n_2 T_2}{n_1 + n_2} \quad (23)$$

$$T_{RMS} = \frac{n_1 T_1^{3/2} + n_2 T_2^{3/2}}{n_1 T_1^{1/2} + n_2 T_2^{1/2}} \quad (24)$$

where  $n_1$ ,  $n_2$ ,  $T_1$ , and  $T_2$  are the respective densities and temperatures of the two components of the spectrum.

A single monoenergetic beam can match two velocity moments of the distributed spectrum if its density and energy are chosen according to equations (12)-(15) above. For example, if the beam density is equal to the total plasma density,  $n_1 + n_2$ , and its energy is  $3/2 T_{AV}$ , then the zeroth and second velocity moments of the two-Maxwellian plasma and the monoenergetic beam are equal.

Two methods exist for matching the velocity moments of a two-Maxwellian distribution by two monoenergetic beams. First, the energy and density of each beam can be chosen individually to match two moments of each of the Maxwellian components of the spectrum. In this case, equations (12)-(15) would be employed along with the densities and temperatures of the two-Maxwellian fit.

The second approach is to use the average and RMS temperatures of the two-Maxwellian fit, equations (23) and (24), and to calculate the beam velocities and densities from equations (18) and (18). In both cases, as many as four moments of the two-Maxwellian distribution function can be matched by two monoenergetic beams. In practical situations, physical considerations would be required to make a choice between the two methods of matching velocity moments.

The moments of a two-Maxwellian distribution function can be matched in several different combinations with multiple monoenergetic beams. As in the two-beam case, each Maxwellian component of the plasma can have one or more beams assigned to it which individually match velocity moments. For six-moment matching, three beam energies and densities could be selected using equation (22) for each component, and a total of six beam energies would be required to simulate the two-Maxwellian plasma. As mentioned above, the computed values of the zeroth through fifth moment of the full spectrum can also be used directly to find three beam energies and densities through the iterative minimization procedure.

### Arbitrarily Assigned Beam Energies

The velocity moments of a measured distribution function can also be matched by monoenergetic beams whose velocities are chosen arbitrarily. When the beam velocities are fixed, then it is only a matter of solving a set of linear simultaneous equations for the beam densities. It should be pointed out that not all combinations of beam velocity may be chosen, because negative, and therefore unphysical, solutions for the beam densities can be obtained in some cases. In other cases, the envelope of beam densities is far from being a smooth function of the beam velocity spectrum. The unphysical and intuitively unsatisfying results using arbitrarily assigned beam energies cast doubt on the usefulness of this approach to match velocity moments of distributed spectra.

## SPACECRAFT CHARGING CALCULATIONS

The previous section presented some mathematical techniques to relate the characteristics of undisturbed plasmas to those of one or more monoenergetic beams of charged particles. It was assumed that the plasma or beams produced a flux of particles at a given surface, although no interactions between the particles and the surface were considered.

In this section we shall compare the electrostatic charging produced by plasmas and various combinations of monoenergetic electron and ion beams using a model which accounts for several of the interactions between the incident charged particles and a "typical" spacecraft. The spacecraft charging calculations are, of course, only one of several possible approaches for making a qualitative comparison of the effects of plasmas and combinations of monoenergetic beams. A spacecraft simulation facility, however, will devote a considerable amount of its effort to the study of the effects of electrostatic charging, and this choice for comparison can be justified on these grounds.

## CHARGING MODEL

The spacecraft charging model developed by Garrett<sup>(10)</sup> calculates the equilibrium potential of a surface which receives isotropic fluxes of electrons and ions with arbitrary energy spectra and which loses charge by secondary electron emission, electron backscatter, and photoelectric emission. The model has been rather successful in predicting the potential of high-altitude satellites instrumented to measure the differential energy spectra of electrons and protons in geomagnetic substorm plasmas<sup>(11)</sup>.

The model assumes that the spacecraft can be represented as a spherical Langmuir probe in a plasma whose Debye length is much greater than the dimensions of the probe. The energy spectra of the plasma electrons and ions are divided into 62 energy "bins", and the flux of charged particles to the surface calculated, taking into account the electrostatic potential of the satellite and conservation of mass. Maxwellian, two-Maxwellian, and arbitrary spectra observed from the spacecraft's instrumentation can be loaded into the energy bins.

Secondary electron emission from electron and ion bombardment and electron backscatter are calculated as a function of the incident particle flux and the measured energy dependence of the secondary emission and backscatter coefficients of aluminum. Corrections for the heterogeneous surface of an actual spacecraft are made by small adjustments of these coefficients to bring the calculated potential of the satellite equal to its measured value when the satellite is in "typical" plasma conditions. Charge losses by photoemission are included by an empirical formula.

We have modified the model in two ways. First, the time dependence of charging was included by representing the satellite as an isolated spherical capacitor. The amount of charge gained and lost by the surface is calculated for short increments of time in which the potential is held constant. The net gain of charge is then used to compute the new value of potential to be used during the following time increment. This procedure is repeated until the potential of the model satellite does not vary in succeeding increments of time.

The second modification was used only for potential calculations of the model when irradiated by monoenergetic, initially parallel beams of noninteracting charged particles. It accounts for the electrostatic deflection of the beams in the electric field of the charged body which attracts oppositely charged particles and repels particles of the same sign.

The total current to a surface of arbitrary shape in a parallel beam is simply the product of the current density,  $j$ , and the geometric cross section,  $A$ , in a plane perpendicular to the current density vector. If the initially parallel beam is deflected by a symmetrical potential well, the deflection can be represented as an "effective" cross-sectional area which depends on the strength of the field and the kinetic energy and charge of the particles. The effective area of a spherical conductor of radius  $R$  is,

$$\begin{aligned}
A_{\text{eff}} &= \pi R^2 \left( 1 - \frac{q\varphi_s}{|qE|} \right) & (q\varphi_s < |qE|) \\
A_{\text{eff}} &= 0 & (q\varphi_s > |qE|)
\end{aligned}
\tag{25}$$

where  $\varphi_s$  is the (signed) potential of the sphere, and  $q$  and  $E$  are the (signed) charge and initial kinetic energy of the incident charged particles.

For the charging calculations, the electron and ion current to the model satellite was set equal to the sum of the currents from the monoenergetic beams, each of which was given by  $I_i = j_i A_{\text{eff}}$  where  $j_i$  is the unperturbed current density of the  $i^{\text{th}}$  beam with energy  $E_i$ .

The secondary emission current from electron and ion bombardment and the electron backscattering were calculated as a function of the energy of the incident particles by the same subroutines used by Garrett's model for distributed energy spectra. No photoemission was included in the spacecraft charging calculations in order to simplify comparison of the results between monoenergetic beams and distributed spectra.

## Results

The spacecraft charging model was used to calculate the potential of a spherical satellite with a radius of 1 meter and initial potential of zero. The charging by plasmas with several different electron and ion temperatures were compared to charging by beams whose energies and current densities were selected by the methods discussed above. Table 2 presents the parameters of some of the Maxwellian plasmas and beams and for the charging calculations.

Charging by single monoenergetic electron and proton beams and Maxwellian plasma was computed for several beam energies and plasma temperatures. The current densities and energies were selected so that the first (number flux) and third (energy flux) velocity moments of the monoenergetic beams matched those of the Maxwellian plasmas, equations (14) and (15). For this case, the beam energies were twice the corresponding plasma temperature.

$$\begin{aligned}
E_b &= 2 kT \\
j_b &= qn \sqrt{\frac{kT}{2\pi m}}
\end{aligned}
\tag{25}$$

where  $n$  and  $T$  are the density and temperature of the Maxwellian plasma component,  $q$  and  $m$  are the charge and mass of the plasma and beam particles (assumed the same species), and  $E_b$  and  $j_b$  are the undisturbed energy and current density of the beam.

Figure 1 shows the charging of the model satellite with a radius of 1 meter under irradiation by single 20 keV electron and proton beams and by a hydrogen plasma in which the electron and ion temperatures are 10 keV. It can be seen that the charging rate and equilibrium potential of the satellite is higher when exposed to the monoenergetic beams, although some differences are to be expected because of the important influence of the secondary electron emission coefficients on the charging process.

The equilibrium potentials found from calculations of charging by Maxwellian plasma and beams with energies and current densities given by equation (25) are compared in figure 2. The correspondence is surprisingly good, considering the crudeness of simulating a Maxwellian velocity distribution by a single monoenergetic beam.

Figure 3 shows calculations of charging by a Maxwellian plasma with an electron temperature of 10 keV and an ion (proton) temperature of 20 keV. Charging by electron beams with an energy of 20 keV and proton beams of 40 keV and current densities for each component given by equation (25) are also shown. In this case, the equilibrium potential in the Maxwellian plasma is somewhat higher than under irradiation by the beams.

The energies and densities required for two beams to match four velocity moments of a Maxwellian plasma are given in equations (20) and (21). We have calculated the charging by two electron and proton beams and in Maxwellian plasmas.

Figure 4 shows the results of the calculations for electron and ion beams with energies of 5.69 keV and 30.1 keV and for a Maxwellian plasma with electron and ion temperatures of 10 keV. The equilibrium potential of the satellite model is more than 2 kV greater for charging by the beams than by the plasma, although the charging rate is about equal for both cases from 0 to 0.05 seconds.

Charging by three monoenergetic electron and three monoenergetic electron and ion beams whose velocity moments match six moments of a Maxwellian plasma was computed using the spacecraft charging model. The beam energies and currents were found from equations (22) to match the velocity moments of a Maxwellian hydrogen plasma with an electron and ion temperature of 10 keV.

The results of the charging calculations are shown in figure 5. There is very close agreement between the charging rates and equilibrium potentials for both the three-beam and Maxwellian plasma cases.

The charging of the satellite model was calculated using beams chosen to simulate the differential energy spectrum of the current density of a Maxwellian plasma. As discussed above, the energy distribution was broken into four parts and the current density and average energy of each part computed, using equations (2) and (4).

Figure 6 shows the charging using the four-beam solution given in Table 1 compared with charging by a Maxwellian plasma with electron and ion temperatures of 10 keV. It is somewhat surprising that the equilibrium potential found with four electron and ion beams chosen to mimic the spectral shape of the Maxwellian plasma is not as close as with other cases with fewer beams.

### Beams and Two-Maxwellian Plasma

The velocity distribution of a non-Maxwellian plasma can be approximated by a two-Maxwellian distribution function, each component of the distribution being characterized by a temperature and a particle density. We have computed the charging of the satellite model in a plasma with a two-Maxwellian electron distribution function and single-Maxwellian ions. The two electron components have temperatures of 10 keV and 30 keV, and densities of  $3.0 \text{ cm}^{-3}$  and  $0.43 \text{ cm}^{-3}$ , respectively. The proton plasma has a temperature of 10 keV and has a number density equal to the total electron density.

We have compared the charging by the two-Maxwellian plasma to that of several combinations of monoenergetic beams. Table 3 shows the beam energies, current densities, and resultant equilibrium potential of the satellite model.

The equilibrium potential found with a single electron beam is presented to show the effect of removing ions from the simulation. Without the ion component, the satellite model charges until the secondary electron emission and backscatter are equal to the incident electron flux. The equilibrium potential is close to that of the electron beam because the secondary electron emission coefficient peaks at an energy of a few hundred electronvolts<sup>(10)</sup> and is small at higher energies.

The single-electron and single-ion beam energies and currents in Table 3 were chosen to match two velocity moments of the two-Maxwellian plasma. The two-electron and single-ion beam energies and currents match the first and third velocity moments (particle and energy flux) of each component of the distribution functions.

The energies and currents of the two-electron and two-ion beam case were found, using equations (17) and (18), to match four velocity moments of the distribution functions, based on the average and RMS temperatures of the plasma particles.

The discrepancies between the calculations of equilibrium potential in the two-Maxwellian plasma and in monoenergetic beams are somewhat greater than those found with a single-Maxwellian plasma. The difference may be caused by the higher temperature component of the electron plasma, which skews the second and third velocity moments of the electron distribution function. The high-energy electron beams required to match these velocity moments apparently have a strong influence on the equilibrium potential of the model.

## DISCUSSION

The calculations give a qualitative idea of the charging which would be observed in a spacecraft testing facility in which monoenergetic beams were used to simulate space plasmas with distributed energy spectra. As expected, the equilibrium potential of the spacecraft under test, and therefore the charge density on its surface, is only a function of the electron and ion beam energies and currents. An important result, however, is the observation that the monoenergetic beams can be chosen to match several velocity moments of a distributed spectrum and, at the same time, produce the same charge density on the spacecraft. Thus, surface phenomena which are influenced, for example, by energy flux as well as charge density can be investigated in a laboratory facility with a reasonable degree of confidence in the simulation fidelity.

It should be made clear that the charging model used here is a very simple one and does not account for the complex geometry or surface details of a real spacecraft. More complicated charging codes exist, however, which could be used to make more detailed comparisons of spacecraft charging by monoenergetic beams and space plasmas. The NASCAP code<sup>(12)</sup>, for example, is probably the most ambitious attempt to represent the geometrical and surface configuration of real satellites in the environment of geosynchronous orbit. Modifications of NASCAP would be required to calculate the charging of a three-dimensional object under irradiation by beams of charged particles, but it is likely that NASCAP would be a useful tool for comparing the conditions of laboratory simulation to those of space.

The author gratefully acknowledges the significant contributions to the work reported here by Betty A. Reid, Stephen N. Bunker and Steven H. Face.

## REFERENCES

1. A. Rosen, editor, Spacecraft Charging by Magnetospheric Plasmas, (M.I.T. Press, Cambridge, Massachusetts, 1975).
2. C.P. Pike and R.R. Lovell, editors, Proc. of the Spacecraft Charging Technology Conference, Report No. AFGL-TR-77-0051, Air Force Geophysics Laboratory, Hanscom AFB, Mass., 1977.
3. R.C. Finke and C.P. Pike, editors, Spacecraft Charging Technology - 1978, NASA Conference Publication 2071, NASA Lewis Research Center, Cleveland, Ohio, 1979.
4. F.D. Berkopoc, N. John Stevens, and J.C. Sturman, "The Lewis Research Center Geomagnetic Substorm Simulation Facility", Report No. NASA TM X-73602, NASA Lewis Research Center, Cleveland, Ohio, 1976.
5. O.L. Pearson, "Modification of a Very Large Thermal-Vacuum Test Chamber for Ionosphere and Plasmasphere Simulation", American Institute of Aeronautics and Astronautics, Inc., New York, Paper 78-1625, 1978.

6. W. Halverson, "Modifications of Ionospheric Simulation Capability. Volume 1: Study", Report No. FR-60021, Spire Corporation, Bedford, Massachusetts, 1979.
7. H.B. Garrett, E.G. Mullen, E. Ziemba, and S.E. DeForest, "Modeling of the Geosynchronous Orbit Plasma Environment - Part 2", Report No. AFGL-TR-78-0304, Air Force Geophysics Laboratory, Hanscom AFB, Massachusetts, 1978.
8. P.R. Bevington, Data Reduction and Error Analysis for the Physical Sciences (McGraw-Hill Book Company, New York, 1969), Ch. 11.
9. H.B. Garrett, "Modeling of the Geosynchronous Orbit Plasma Environment - Part 1", Report No. AFGL-TR-77-0288, Air Force Geophysics Laboratory, Hanscom AFB, Massachusetts, 1977.
10. H.B. Garrett, "Spacecraft Potential Calculations - A Model", Report No. AFGL-TR-78-0116, Air Force Geophysics Laboratory, Hanscom AFB, Mass., 1978.
11. H.B. Garrett and S.E. DeForest, *J. Geophys. Res.* 84, 2083 (1979).
12. I. Katz, J.J. Cassidy, M.J. Mandell, G.W. Schnuell, P.G. Steen, and J.C. Roche, "The Capabilities of the NASA Charging Analyzer Program", Spacecraft Charging Technology - 1978 (see Ref. 3).

TABLE 1. PIECEWISE REPRODUCTION OF MAXWELLIAN SPECTRUM BY FOUR BEAMS

Maxwellian Temperature = 10 keV		
Energy Boundaries $E_1, E_2$ (keV)	Normalized Current Density $j(E_1, E_2)/j_0$	Beam Energy $E(E_1, E_2)$ (keV)
0, 7.5	0.173	4.682
7.5, 15	0.269	11.20
15, 30	0.359	21.49
30,	0.199	42.53

**TABLE 2. SPACECRAFT CHARGING BY MAXWELLIAN  
PLASMAS AND MONOENERGETIC BEAMS**

PLASMA		
Electrons:	$T_e = 10 \text{ keV}, j_e = 1.0 \text{ nA/cm}^2$	$\phi_{eq} = -12.5 \text{ kV}$
Ions:	$T_i = 10 \text{ keV}, j_i = 0.023 \text{ nA/cm}^2$	
Electrons:	$T_e = 10 \text{ keV}, j_e = 1.0 \text{ nA/cm}^2$	$\phi_{eq} = -14.2 \text{ kV}$
Ions:	$T_i = 20 \text{ keV}, j_i = 0.033 \text{ nA/cm}^2$	
BEAMS		
1 Electron:	$E_e = 20 \text{ keV}$ $j_e = \text{nA/cm}^2$	$\phi_{eq} = -13.5 \text{ kV}$
1 Ion:	$E_i = 20 \text{ keV}$ $j_i = 0.023 \text{ nA/cm}^2$	
1 Electron:	$E_e = 20 \text{ keV}$ $j_e = 1.0 \text{ nA/cm}^2$	$\phi_{eq} = -12.9 \text{ kV}$
1 Ion:	$E_i = 40 \text{ keV}$ $j_i = 0.033 \text{ nA/cm}^2$	
2 Electron:	$E_{e1} = 5.69 \text{ keV}$ $j_{e2} = 0.41 \text{ nA/cm}^2$ $E_{e2} = 30.1 \text{ keV}$ $j_{e2} = 0.59 \text{ nA/cm}^2$	$\phi_{eq} = -15.0 \text{ kV}$
2 Ion:	$E_{i1} = 5.69 \text{ keV}$ $j_{i1} = 0.0096 \text{ nA/cm}^2$ $E_{i2} = 30.1 \text{ keV}$ $j_{i2} = 0.014 \text{ nA/cm}^2$	
3 Electron:	$E_{e1} = 3.03 \text{ keV}$ $j_{e1} = 0.16 \text{ nA/cm}^2$ $E_{e2} = 16.6 \text{ keV}$ $j_{e2} = 0.67 \text{ nA/cm}^2$ $E_{e3} = 49.6 \text{ keV}$ $j_{e3} = 0.17$	$\phi_{eq} = -11.9 \text{ kV}$
3 Ion:	$E_{i1} = 3.03 \text{ keV}$ $j_{i1} = 0.0037 \text{ nA/cm}^2$ $E_{i2} = 16.6 \text{ keV}$ $j_{i2} = 0.016 \text{ nA/cm}^2$ $E_{i3} = 49.6 \text{ keV}$ $j_{i3} = 0.0040 \text{ nA/cm}^2$	

TABLE 3. SPACECRAFT CHARGING BY TWO-MAXWELLIAN PLASMA AND MONOENERGETIC BEAMS

PLASMA		
Electrons:	$T_{e1} = 10 \text{ keV}, j_{e1} = 0.8 \text{ nA/cm}^2$ $T_{e2} = 30 \text{ keV}, j_{e2} = 0.2 \text{ nA/cm}^2$ $(T_e)_{AV} = 12.52 \text{ keV}$ $(T_e)_{RMS} = 14.0 \text{ keV}$	$\phi_{eq} = -14.0 \text{ kV}$
Ions:	$T_i = 10 \text{ keV}, j_i = 0.021 \text{ nA/cm}^2$	
BEAMS		
1 Electron	$E_e = 2(T_e)_{RMS} = 28.0 \text{ keV}$	$\phi_{eq} = -26.8 \text{ kV}$
1 Electron	$E_e = 3/2 (T_e)_{AV} = 18.8 \text{ keV}$ $j_e = 1.1 \text{ nA/cm}^2$	$\phi_{eq} = -12.7 \text{ kV}$
1 Ion	$E_i = 3/2 T_i = 15 \text{ keV}$ $j_i = 0.023 \text{ nA/cm}^2$	
1 Electron	$E_e = 2(T_e)_{RMS} = 28.0 \text{ keV}$ $j_e = 1.0 \text{ nA/cm}^2$	$\phi_{eq} = -19.8 \text{ kV}$
1 Ion	$E_i = 2 T_i = 20 \text{ keV}$ $j_i = 0.021 \text{ nA/cm}^2$	
2 Electron	$E_{e1} = 2 T_{e1} = 20 \text{ keV}$ $j_{e1} = 0.8 \text{ nA/cm}^2$ $E_{e2} = 2 T_{e2} = 60 \text{ keV}$ $j_{e2} = 0.2 \text{ nA/cm}^2$	$\phi_{eq} = -18.2 \text{ kV}$
1 Ion	$E_i = 2 T_i = 20 \text{ keV}$ $j_i = 0.021 \text{ nA/cm}^2$	
2 Electron	$E_{e1} = 7.92 \text{ keV}, j_{e1} = 0.54 \text{ nA/cm}^2$ $E_{e2} = 51.9 \text{ keV}, j_{e2} = 0.46 \text{ nA/cm}^2$	$\phi_{eq} = -19.2 \text{ kV}$
2 Ion	$E_{i1} = 5.69 \text{ keV}, j_{i1} = 0.0096 \text{ nA/cm}^2$ $E_{i2} = 30.07 \text{ keV}, j_{i2} = 0.014 \text{ nA/cm}^2$	

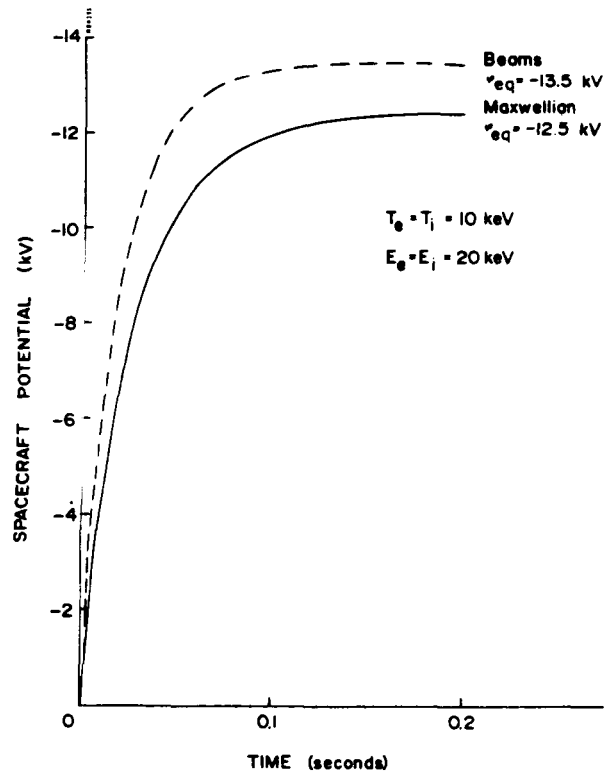


FIGURE 1. SPACECRAFT CHARGING BY 10 keV MAXWELLIAN PLASMA AND 20 keV ELECTRON AND ION BEAMS

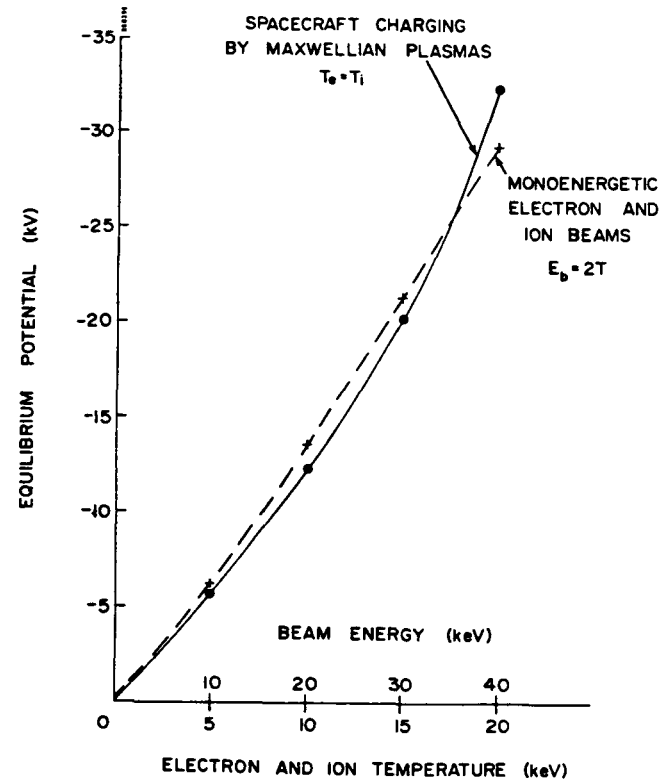


FIGURE 2. EQUILIBRIUM POTENTIAL IN MAXWELLIAN PLASMAS AND SINGLE ELECTRON AND ION BEAMS

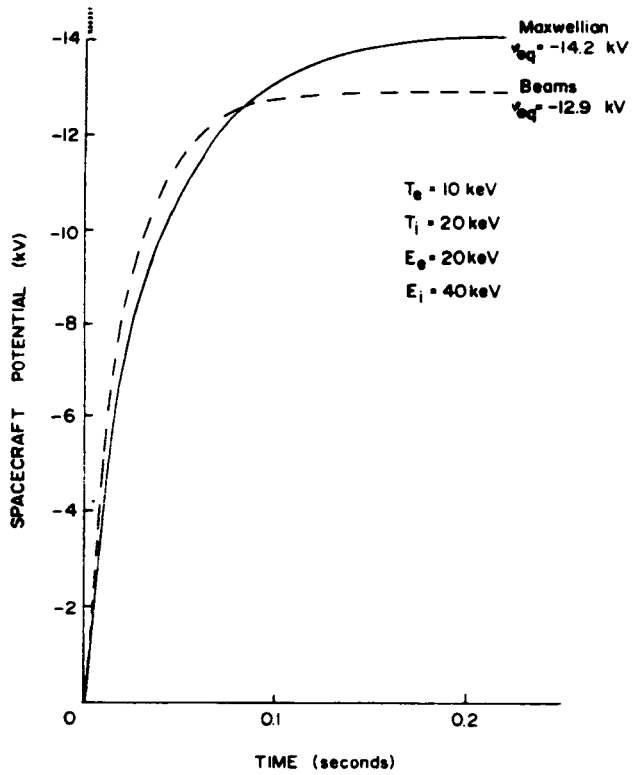


FIGURE 3. CHARGING BY MAXWELLIAN PLASMA ( $T_e = 10$  keV,  $T_i = 20$  keV) AND SINGLE ELECTRON AND ION BEAMS

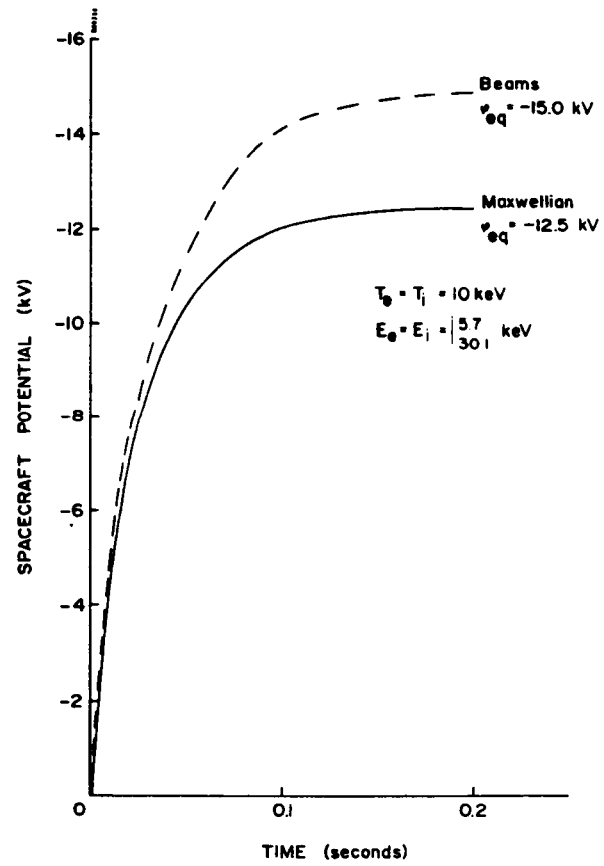


FIGURE 4. CHARGING BY MAXWELLIAN PLASMA AND TWO ELECTRON AND ION BEAMS

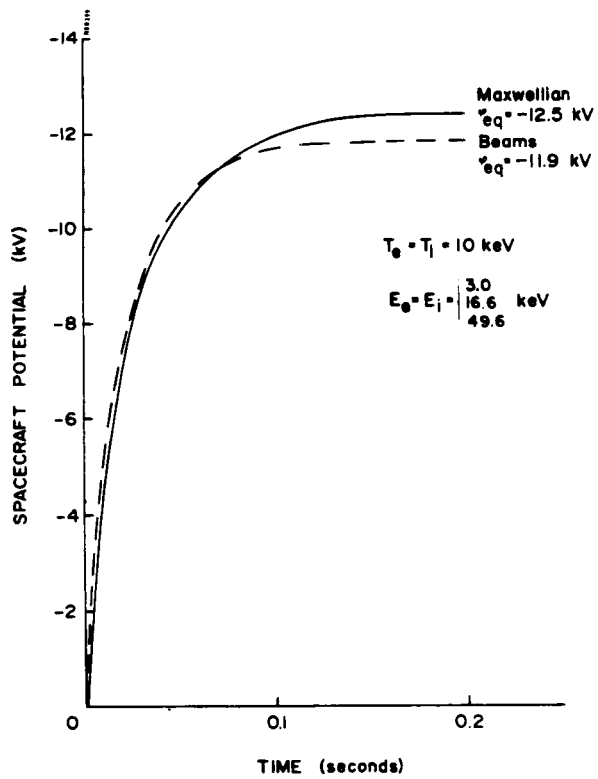


FIGURE 5. CHARGING BY MAXWELLIAN PLASMA AND THREE ELECTRON AND ION BEAMS

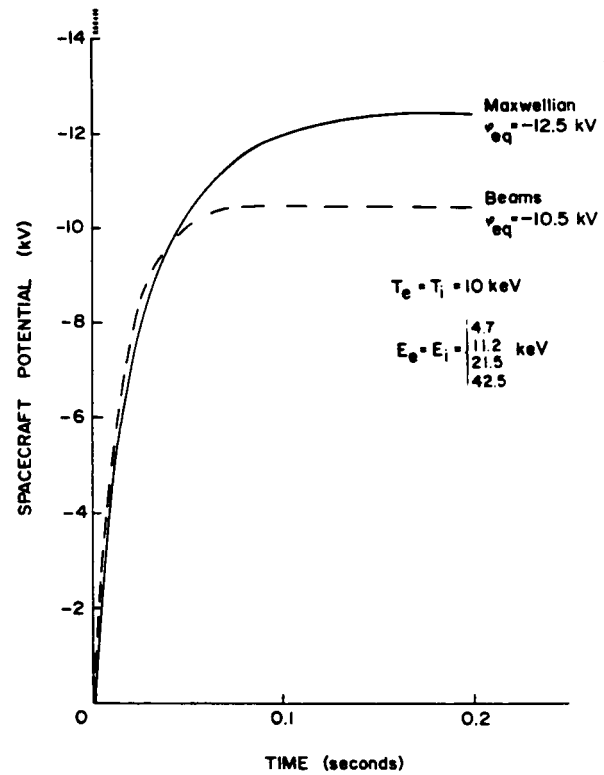


FIGURE 6. CHARGING BY MAXWELLIAN PLASMA AND FOUR ELECTRON AND ION BEAMS